Journal of Hazardous Materials 185 (2011) 124–130

Contents lists available at ScienceDirect

Journal of Hazardous Materials

journal homepage: www.elsevier.com/locate/jhazmat

Electrospun nylon-6 spider-net like nanofiber mat containing TiO_2 nanoparticles: A multifunctional nanocomposite textile material

Hem Raj Pant[a,b], Madhab Prasad Bajgai[c], Ki Taek Nam[d], Yun A. Seo[d], Dipendra Raj Pandeya[e], Seong Tshool Hong[e], Hak Yong Kim[d,*]

[a] Department of Bionanosystem Engineering, Chonbuk National University, Jeonju 561-756, Republic of Korea
[b] Department of Engineering Science and Humanities, Institute of Engineering, Pulchowk Campus, Tribhuvan University, Kathmandu, Nepal
[c] Department of Pathology, University of British Columbia, Vancouver, B.C.V6T1Z3 Canada
[d] Department of Textile Engineering, Chonbuk National University, 664-14, 1Ga, Duckjin-dong, Jeonju 561-756, Republic of Korea
[e] Department of Microbiology and Immunology, Institute for Medical Science, Chonbuk National University Medical School, Jeonju 561-756, South Korea

ARTICLE INFO

Article history:
Received 12 August 2010
Received in revised form 2 September 2010
Accepted 2 September 2010
Available online 15 September 2010

Key words:
Electrospinning
Spider-net
Antimicrobial
Nanocomposite
Nylon-6/TiO_2

ABSTRACT

In this study, electrospun nylon-6 spider-net like nanofiber mats containing TiO_2 nanoparticles (TiO_2 NPs) were successfully prepared. The nanofiber mats containing TiO_2 NPs were characterized by SEM, FE-SEM, TEM, XRD, TGA and EDX analyses. The results revealed that fibers in two distinct sizes (nano and subnano scale) were obtained with the addition of a small amount of TiO_2 NPs. In low TiO_2 content nanocomposite mats, these nanofiber weaves were found uniformly loaded with TiO_2 NPs on their wall. The presence of a small amount of TiO_2 NPs in nylon-6 solution was found to improve the hydrophilicity (antifouling effect), mechanical strength, antimicrobial and UV protecting ability of electrospun mats. The resultant nylon-6/TiO_2 antimicrobial spider-net like composite mat with antifouling effect may be a potential candidate for future water filter applications, and its improved mechanical strength and UV blocking ability will also make it a potential candidate for protective clothing.

1. Introduction

Recently, the synthesis and design of organic–inorganic hybrid materials have generated great interests in the fields of material sciences. Composite nanofiber materials formed by blending nano-sized inorganic and organic materials are attractive for the purpose of creating new materials with new or enhanced properties compared with single organic or inorganic materials. The incorporation of a small amount of inorganic nanoparticles can improve the performance of the mechanical, thermal, optical, electrical, antimicrobial, antifouling and catalytic properties of a polymer matrix [1–4]. This process makes fibers the best candidate in many applications such as filtration [3,4], the manufacturing of protective clothing [5,6], tissue engineering [7,8], and sensors [9]. Different methods, such as sol–gel processing, dip-coating, spin-coating, and evaporation–deposition, have been used to incorporate inorganic nanoparticles into a polymer matrix [10–12]. Electrospinning is regarded as a simple and versatile method for this process [13]. Furthermore, polymeric fiber mats with nano and subnano fibers (spider-net like structure) in the same mat can attain new properties for the production of high aspect ratio materials. Different researchers have reported the formation of such spider-net like structure nanofiber polymeric mats [14,15]. We successfully synthesized hybrid mats of methoxy poly(ethylene glycol) and nylon-6 as well as poly(acrylic acid) and nylon-6 in the form of a spider-net like structure [16,17]. Nylon-6, PVA and PU polymeric nanofiber mats containing spider-net like structures have been synthesized by the addition of different inorganic salts [18].

Nylon-6 is a biodegradable and biocompatible polymer. It is widely used in many industrial fields for its low cost, superior fiber forming ability, good mechanical strength, and strong chemical and thermal stabilities [19]. Electrospun nylon-6 mats have been reported as effective water filtration media [20]. Furthermore, electrospun nylon-6 mats in the spider-net like structure with improved hydrophilicity might be a potential candidate for this application. Nano TiO_2 is well known for its many advantages, such as good stability, hydrophilic properties, UV blocking ability and excellent photocatalytic and antimicrobacterial capacity [21,22]. Photocatalytic degradation using TiO_2 NPs is widely studied, because it efficiently converts abundant UV–visible light energy into chemical energy, which is used to decompose harmful organic materials in air and water [23–25]. UV illumination of TiO_2 excites electrons from the valence band to the conduction band, leaving holes in the valence band. The electrons then react with oxygen

* Corresponding author. Tel.: +82 632 7023 51; fax: +82 632 7042 49.
E-mail address: khy@jbnu.ac.kr (H.Y. Kim).

0304-3894/$ – see front matter © 2010 Elsevier B.V. All rights reserved.
doi:10.1016/j.jhazmat.2010.09.006

molecules to produce superoxide anions where as the holes react with water to produce hydroxyl radicals. These two highly reactive species are able to decompose a variety of organic toxic materials [23].

The mixing of these two materials at the nanoscale can form a unique and effective multifunctional nanocomposite textile material. We expect that the TiO_2 NPs can form spider-net like electrospun nylon-6 fiber mats, which can lead to a remarkable increase in the number of reactive sites with a corresponding improvement in hydrophilicity, photocatalytic and antimicrobial activity. Here, we reported our recent focus on the preparation of a novel nylon-6/TiO_2 organic–inorganic nanocomposite material in the form of an electrospun mat, containing two distinct types of fibers (nano- and subnano-sized) loaded with TiO_2 NPs, with superior mechanical strength, high hydrophilicity, and good antimicrobial as well as UV blocking ability. This spider-net like nano-structure mat with antimicrobial and hydrophilic properties (antifouling effect) would have great potentiality for water filter applications. Furthermore, the good UV blocking capacity and improved mechanical strength of electrospun mat is highly beneficial for different kinds of protective clothing.

2. Experimental procedure

2.1. Preparation of composite Nylon-6/TiO2 mats

Nylon-6/TiO_2 hybrid nanocomposite mats were prepared by mixing different amounts (1, 5 and 10 wt%) of TiO_2 NPs (Aeroxide P25, 80% anatase 20% rutile, average particle size of 21 nm and specific surface area of $50 \pm 15\ m^2\ g^{-1}$) with a 20 wt% nylon-6 (KN20 grade, Kolon, Korea) solution prepared in a 4:1 ratio by weight of formic acid and acetic acid (Showa, Japan). During electrospinning, the applied voltage was held constant at 18 kV, and the distance between the polymer solution and the polyethylene foil collection screen was kept at 16 cm. After vacuum drying for 24 h, the fiber mats were used for further analysis.

2.2. Characterization

The surface morphology of nanofibers was studied by using scanning electron microscopy (JSM-5900, JEOL, Japan) and field-emission scanning electron microscopy (FE-SEM, S-7400, Hitachi, Japan). Information about the phase and crystallinity was obtained by using a Rigaku X-ray diffractometer (XRD, Rigaku, Japan) with Cu K_α (λ = 1.540 Å) radiation over the Bragg angle ranging from 10° to 80°. High-resolution images of nanofibers containing TiO_2 NPs were obtained via transmission electron microscopy (TEM, JEM-2010, JEOL, Japan) operating at 200 kV.The thermal properties of composite mats were measured by a thermogravimetric analyzer (Perkin–Elmer Inc., TGA 6, USA). The conductivity was measured by an EC meter CM 40G Ver. 1.09 (DKK, TOA, Japan) and the viscosity of the solution was measured by a Brookfield, DV-III ultra programmable Rheometer at room temperature.

2.3. Mechanical strength measurement

Using an Instron mechanical tester (LLOYD instruments, LR5K plus, UK) in tensile mode, the mechanical properties of the as-spun mats were measured. The specimen thicknesses were measured using a digital micrometer with a precision of 1 μm. The extension rate was 5 mm/min at room temperature and 5 specimens with dimensions of 3.5 mm and 940 mm (width and length) were tested and averaged for each fiber mat.

2.4. Contact angle measurement

The wettability of the electrospun mats was measured with deionized water contact angle measurements using a contact angle meter (GBX, Digidrop, France). Deionized water was automatically dropped (drop diameter 6 μm) onto the mat. The measurement was carried out at 1, 3 and 9 s.

2.5. UV blocking test

The UV blocking ability of nanocomposite mats was evaluated by using a UV–visible spectrometer (Lambda 900, Perkin–Elmer, USA) in the 200–800 nm range. The nanofibers mats of 5 cm × 5 cm in size (about 0.032 mm thick) were directly used for testing. The spectra obtained by using the reflection percentage verses wavelength were used to compare the UV blocking capacity of the composite mats.

2.6. Antimicrobial test

The antibacterial efficiency of nylon-6/TiO_2 nanocomposite mats was quantitatively evaluated using a gram-negative bacterium *Escherichia coli* (*E. coli*) ATCC 52922 as model organism. The bacterial inoculum was prepared in Luria Bertani (LB) nutrient broth (pH = 7) containing 10 g/L of Tryptone Peptone, 5 g/L of Bacto Yeast extract and 5 g/L of NaCl at 37 °C for 12 h. The *E. coli* culture in LB medium was washed by centrifuging at 10,000 × *g* rpm for 1 min and then re-suspended and diluted in distilled water. The electrospun mats of the same diameter were cut and placed at the bottom of the Petri dish, and the *E. coli* suspension of 5.4×10^8 CFU/mL was placed over the mats. The experiments were carried out in the dark and under UV light (15 W). By taking the samples at different intervals of time, the *E-coli* concentration in CFU/mL was evaluated by the plating technique. The number of viable *E. coli* cells was determined by plating onto the LB agar plate and counting colonies after 12 h of incubation at 37 °C.

3. Results and discussion

3.1. Morphology of electrospun mats

During the electrospinning process, an electrified polymeric nylon-6 solution with TiO_2 NPs was extruded through a spinneret and collected as a mat on the rotating drum. The morphologies of the as-prepared electrospun nylon-6 mats with different amounts of TiO_2 are shown in Figs. 1 and 2. From these images, it is clear that the pristine nylon-6 mat does not contain any spider-net like structure, but, with 1% TiO_2, it has a highly interconnected spider-net like structure (Fig. 1b). The formation of the spider-net like structure may be due to the increased ionization of the polymer solution in the presence of TiO_2 during electrospinning. Nylon-6 is a polyelectrolyte. Therefore, its acidic solution may be further ionized in the presence of a small amount of TiO_2 nanoparticles, which is also supported by our conductivity data (Table 1). The good dispersion of TiO_2 up to 1% can decrease the strength of the intermolecular hydrogen bonds between polymeric species (ionized or unionized), making ions free to move, and as a result the conductivity is increased while the viscosity is decreased. However, the reverse result was obtained above a 1% TiO_2 solution due to the aggregation of nanoparticles. Based on our conductivity data, we proposed the possible mechanism for the formation of the spider-net structure in low content TiO_2 (up to 1%) nanocomposite mats, as shown in Fig. 3. Formic acid, a polar monoprotic solvent with high dielectric constant, is capable of attacking the lactam of nylon-6 to produce a series of short chain oligomer/monomer ions ($-CONH_2^+-$) [26].

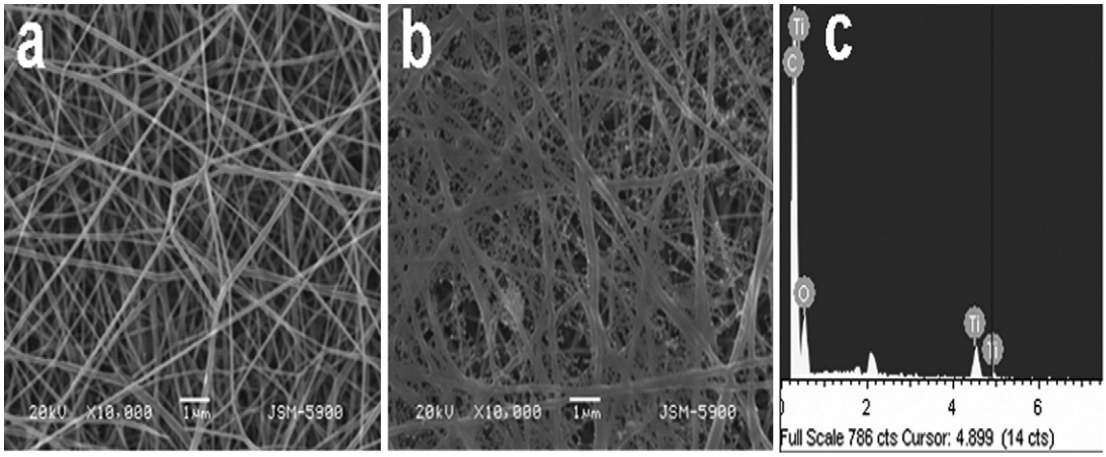

Fig. 1. SEM images: (a) pristine nylon-6, (b) 1% TiO_2 nanocomposite mat of nylon-6 and (c) SEM-EDX of b.

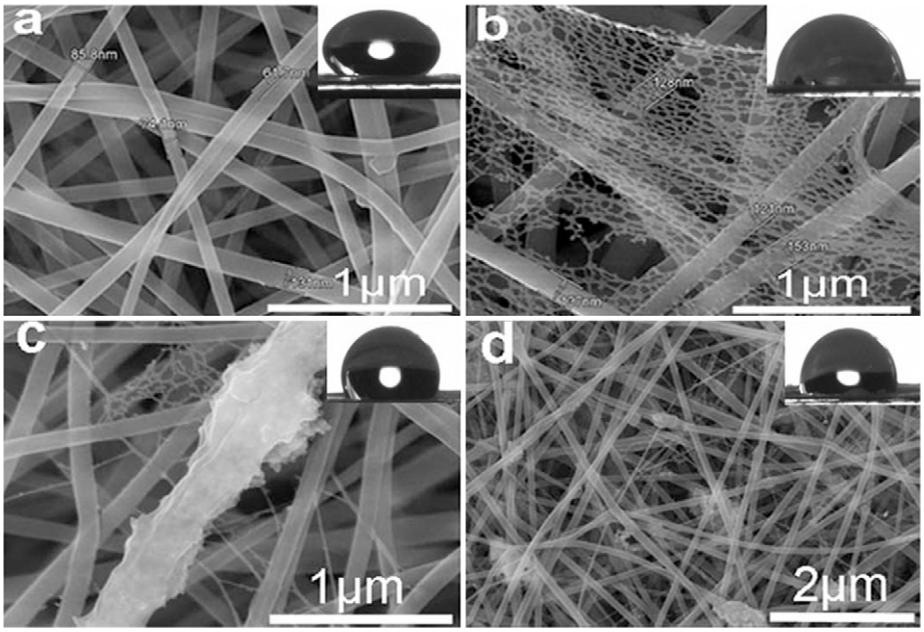

Fig. 2. FE-SEM images: pristine nylon-6 (a) and composite nylon-6/TiO_2 mats containing 1% TiO_2 (b), 5% TiO_2 (c) and 10% TiO_2 (d). Insets are their respective water contact angles at 1 s.

Table 1
Conductivity, viscosity, fiber diameter and water contact angle measurement of different system.

System	Conductivity (mS/m)	Viscosity (cP)	Average fiber diameter (nm)	Water contact angle (degree)		
				1 s	3 s	9 s
Pure solvent	7.1	6	–	–	–	–
Nylon-6 solution/fiber	221.2	1218	110	130.5	122	113
1% TiO_2 in nylon-6 solution/fiber	267.0	1124	130	87	63	43
5% TiO_2 in nylon-6 solution/fiber	210.7	1522	155	111	65	50
10% TiO_2 in nylon-6 solution/fiber	208.4	1648	172	102	72	54

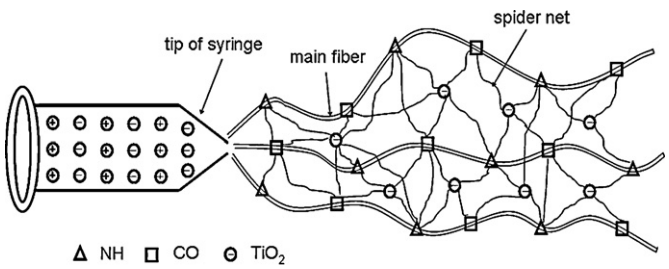

Fig. 3. Schematic illustration showing the mechanism of spider-net like structure formation during electrospinning.

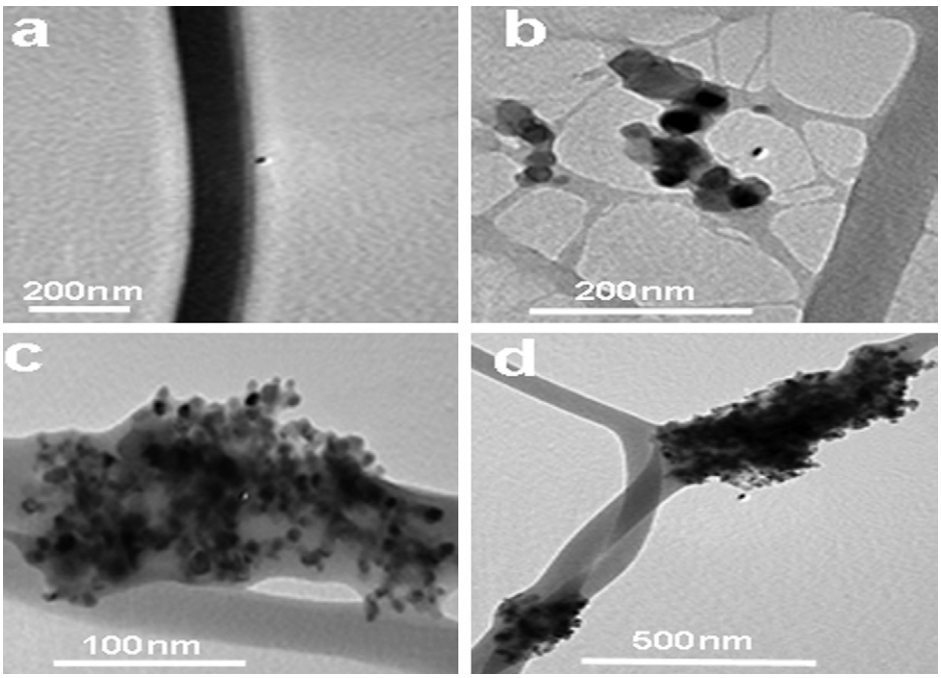

Fig. 4. TEM images: pristine nylon-6 (a) and composite nylon-6/TiO_2 mats containing 1% TiO_2 (b), 5% TiO_2 (c), and 10% TiO_2 (d).

The presence of well-dispersed TiO_2 can further increase the number of ions in the electrospinning solution. A further increase of ions can initiate the splitting up of subnanofibers from the main fibers and solidification with TiO_2 nanoparticles in the form of a spider-net like structure during electrospinning. The CO and NH portion of the ionic species of nylon-6 can hold TiO_2 nanoparticles on the surface of nanofibers. These ionic polymeric species and TiO_2 nanoparticles were connected either by hydrogen bonding or by the formation of complexes with polymer ligands caused by the lone pair of electrons of nitrogen and oxygen. This proposed mechanism is directly evidenced by the TEM results (Fig. 4b), which showed that spider-net fibers issued from the main fibers and almost all TiO_2 nanoparticles were loaded on spider-net fibers.

We observed that the spider-net like structure decreased whereas the fiber diameter slightly increased with increasing amounts of TiO_2 NPs. It is clear from the TEM images (Fig. 4) that with up to 1% TiO_2 NPs in nylon-6/TiO_2 composite mat, the nanoparticles were well-distributed throughout the mat with a continuous spider-net like structure (Fig. 4b). The presence of more than 1% TiO_2 NPs caused the heavily loaded mass on some parts of the nylon-6/TiO_2 composite nanofibers (Fig. 4c and d). It could be explained by the fact that, according to the increasing amount of TiO_2, the nylon-6/TiO_2 spinning solution became more viscous, which could increase the energy needed to overcome surface tension for electrospinning, resulting in more beads-on-string and thicker fibers with rough surfaces, as shown in Fig. 2c and d. To affirm that the TiO_2 was present in the composite mat, SEM-EDX analysis was performed (Fig. 1c), which further confirmed that TiO_2 nanoparticles were loaded on the polymeric nanofibers.

The XRD patterns of nano-sized TiO_2 crystal powders, nylon-6 and nylon-6/TiO_2 composite mats are shown in Fig. 5. The pattern of TiO_2 crystal powders had different crystalline characteristic peaks as shown in Fig. 5a, similar to that reported in the literature [27]. The pattern of the nylon-6/TiO_2 composite mat also had same crystalline characteristic peaks analogous with the characteristic peaks of TiO_2 crystal powders in addition to the γ-phase crystalline peak of nylon-6 at 2θ of 21.25°; nevertheless, their locations occurred with a slight shift compared with the pattern of pure TiO_2 NPs. We observed that the crystalline peak of nylon-6 slightly shifted toward the right whereas the peaks of TiO_2 shifted slightly to the left compared to the peaks for the pure form. This shifting of characteristic peaks of TiO_2 and nylon-6 in the nylon-6/TiO_2 composite mats indicates that there may exist interactions between the polymers and TiO_2 nanoparticles.

The interaction of TiO_2 NPs with nylon-6 in nanocomposite mats was further evaluated via thermogravimetric analysis (TGA) and a differential thermogravimetry (DTG) graph (Fig. 6). A temperature correlation with the maximum thermal degradation rates for pristine nylon-6 at 444.7 °C was observed. The shifting of this value from 444.7 °C in the pristine nylon-6 mat to 447.3 °C in the 1% TiO_2 composite mat (Fig. 6b) indicated the interaction of nanoparticles with the polymer during the formation of the electrospun spider-net like mat. This interaction may be due to the formation of stronger hydrogen bonds between the well-distributed nanoparti-

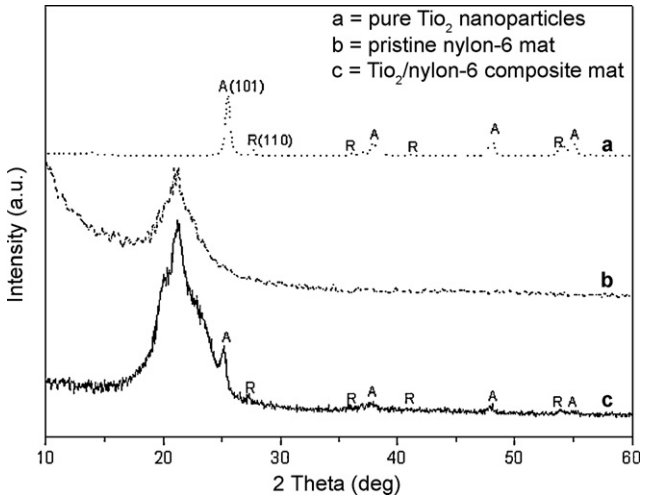

Fig. 5. XRD pattern for pure TiO_2 NPs (a), pristine nylon-6 mat (b) and nylon-6/TiO_2 nanocomposite mat (c).

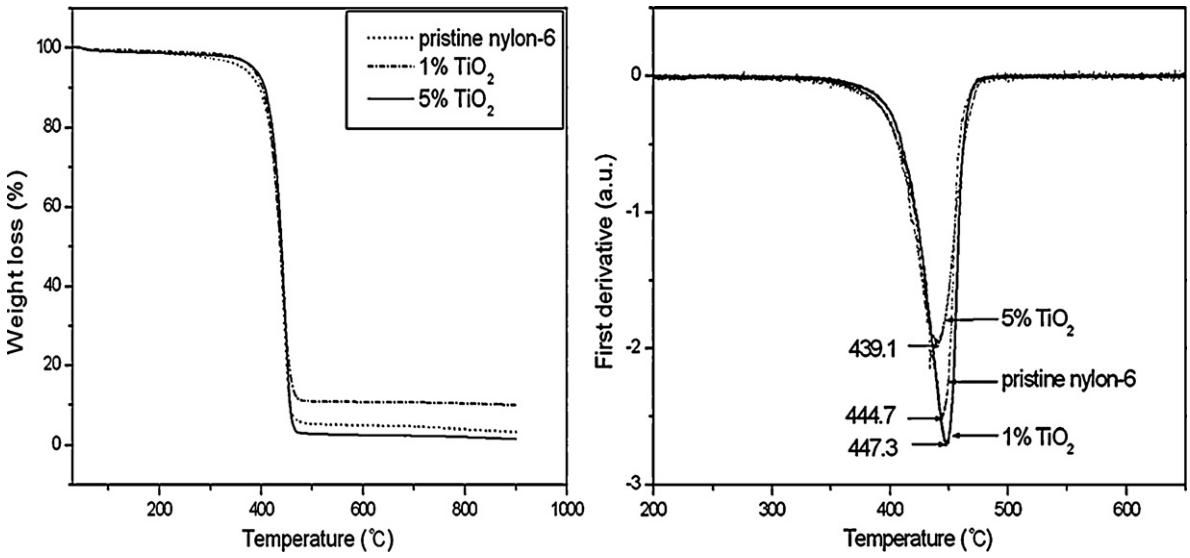

Fig. 6. TGA (a) and DTG (b) curves of pristine nylon-6 and different amount of TiO_2 containing nanocomposite mats.

cles with spider-net like polymer fibers. We obtained the same TGA data for 5% and 10% TiO_2 composite mats as presented in Fig. 6b, with the value of 439.1 °C. This shifting toward lower temperatures may be due to the weakened interconnection force between the polymer chains caused by the aggregation of TiO_2 nanoparticles on the polymer fibers.

3.2. Mechanical strength

The mechanical strength of the nylon-6 nanofiber mat with 1% TiO_2 was found to be greater than that of pure nylon-6, and again it decreased with increasing TiO_2 content (Fig. 7). The enhanced mechanical properties up to 1 wt% TiO_2 may be due to the good dispersion of nanoparticles throughout the polymeric solution as well as the formation of a highly interconnected spider-net like structure (Fig. 2 b). Furthermore, this increased mechanical effect can be attributed to an additional energy-dissipating mechanism introduced by the nanoparticles in nylon-6 due to their good distribution throughout the mat. Molecular dynamics studies suggested that this additional dissipative mechanism is a result of the mobility of the nanoparticles. During the deformation process the nanoparticles may orient and align under tensile stress, creating temporary cross-links between polymer chains and thereby creating a local region of enhanced strength [28]. Therefore, the stress value of the nanocomposite mat with 1% TiO_2 was greater than that of the pristine nylon-6 mat, whereas the strain value of the same mat was less than that of the pristine nylon-6 mat. However, when the size of the nanoparticles increased due to aggregation, as in the 5% and 10% TiO_2 contain mats, they become less mobile. Therefore, the ability of the nanoparticles to dissipate energy was also reduced, resulting in decreased mechanical strength.

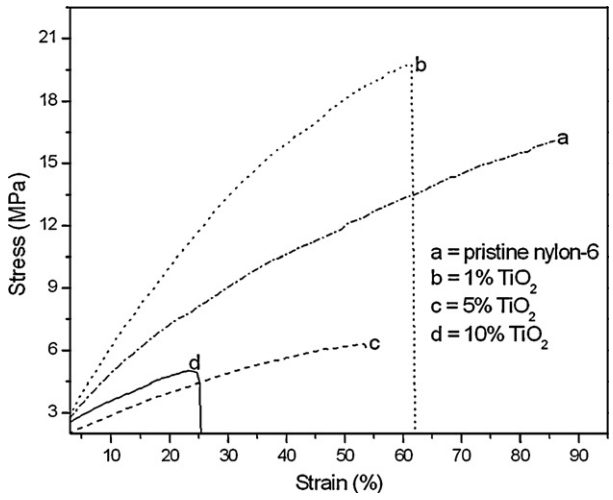

Fig. 7. Typical tensile stress–strain curves of electrospun pristine nylon-6 mat and different amount of TiO_2 contains Nylon-6/TiO_2 nanocomposite mats.

3.3. Water contact angle

The insets of Fig. 2 (a–d) are the water contact angles of the different mats after 1 s for pristine nylon-6, 1, 5 and 10 wt% TiO_2 in composite mats, respectively. It shows that the 1 wt% TiO_2 mat is not only much more hydrophilic than the pure nylon-6 mat but also slightly more hydrophilic than 5 and 10 wt% TiO_2 electrospun mats. It is probably due to the formation of a greater surface to volume ratio of the spider-net like structure as well as well the TiO_2 NPs distributed on them (1 wt% TiO_2 composite mat). The contact angle values of different mats at 1, 3 and 9 s are given in Table 1, which shows that the decreasing rate of the contact angle with time in the nanocomposite mat was much greater than that of pristine nylon-6. The decreased contact angle is an indication of increased hydrophilicity. This increased hydrophilicity can decrease the antifouling effect of filter membranes [29]. Therefore, the presence of TiO_2 NPs in the nylon-6 mat prevents it from fouling. Our results showed that small amount of TiO_2 NPs (1 wt%) in nylon-6 was able to give a spider-net like structure and simultaneously increase the hydrophilicity of the electrospun mat. The presence of the spider-net like structure in the mat not only prevented the passage of the suspended nano impurities of water but also increased the surface energy of the mat to make the mat more hydrophilic. The increased hydrophilicity is responsible for increasing the rate of filtration of water through the mat.

3.4. UV blocking study of composite mats

It is well known that UV light is very harmful for living being. Because of the increasing ozone layer depletion, it cannot block UV rays of sunlight effectively. Therefore, protective clothing capable of blocking UV light has great advantages for this problem. To inves-

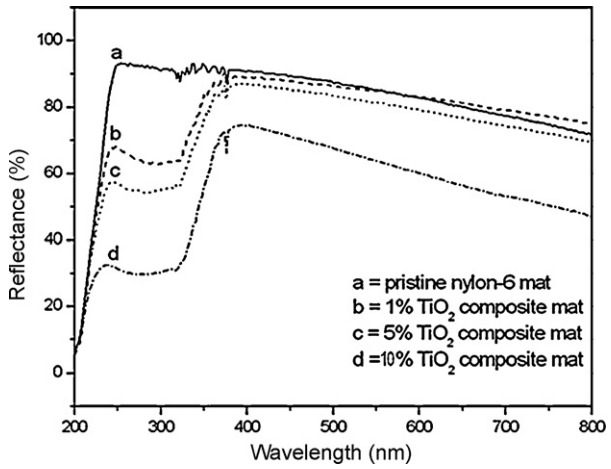

Fig. 8. UV–visible spectra of pristine nylon-6 and different nylon-6/TiO_2 nanocomposite mats.

tigate the UV blocking properties of the nylon-6/TiO_2 fibrous mat, the UV–visible spectra of samples were measured at room temperature. Fig. 8 shows the reflectance spectra of the electrospun pristine nylon-6 mat and those of the three types of electrospun nylon-6 mats with different amounts of TiO_2 NPs. The reflectance decreased as the amounts of TiO_2 in the composite mats increased because of the absorbance of UV light by TiO_2 NPs for transferring the electron from the valance band to the conduction band. Therefore, this novel nylon-6/TiO_2 nanocomposite mat can be used for UV blocking.

3.5. Antibacterial performance

The antimicrobial ability of the nylon-6/TiO_2 composite mats was tested using *E. coli* cell survival under UV light exposure as described in Section 2.6. Fig. 9 shows the antibacterial efficiency of *E. coli* on different 0–10% nylon-6/TiO_2 composite mat surfaces under UV light. To compare the results, a reference *E. coli* solution was kept in the dark. The results showed that almost all the bacterial cells survived in the dark, whereas their survivability was decreased under UV light. The number of cells that survived on pristine nylon-6 was found to be more than that on the nylon-6/TiO_2 composite mats under the same conditions of UV light exposure. It was observed that the survival numbers of bacterial cells decreased

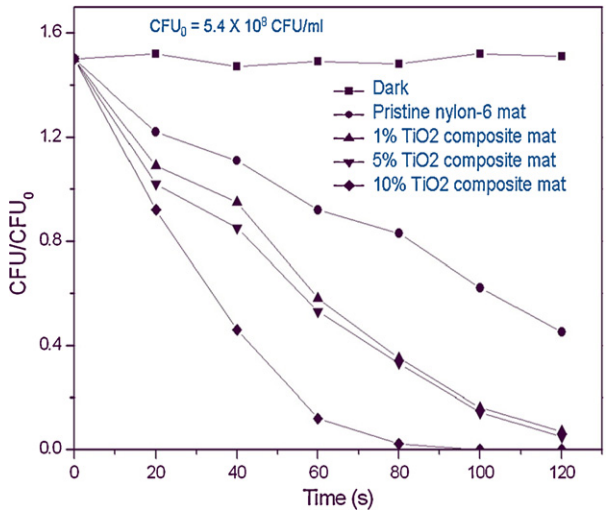

Fig. 9. Antimicrobial efficiency of pristine nylon-6 and different nylon-6/TiO_2 nanocomposite mats.

with increasing amounts of TiO_2 in the composite mats. The similar result in the PVDF membrane containing TiO_2 NPs was also reported by Damodar et al. [3]. Furthermore, we observed that the antimicrobial efficiency of 1% and 5% TiO_2 nanocomposite mats was nearly same (with comparison between 5% and 10% TiO_2 nanocomposite mats) even though the difference in the amount of TiO_2 was a factor of 5 between the two samples. It may be because of the high surface area of TiO_2 NPs provided by the spider-net like structure throughout the 1% TiO_2 nanocomposite mat. These results indicated that the nylon-6/TiO_2 nanocomposite mats exposed to UV light were able to kill *E. coli* cells more efficiently than the pristine nylon-6 mat due to the photocatalytic bactericidal effect of TiO_2 NPs. The bactericidal ability of UV/TiO_2 photocatalysis is due to the presence of different reactive species such as $HO^{\bullet}$, H_2O_2 and $O_2^{\bullet-}$, generated by TiO_2 as well as the direct UV illumination of the cells. Different studies have concluded that the main effective mechanism for the death of *E. coli* cells by bactericidal effect of TiO_2 photocatalysis is $HO^{\bullet}$ attack and the lipid peroxidation reaction [30,31].

4. Conclusion

Nylon-6/TiO_2 composite nanofiber mats were prepared via electrospinning by mixing different amounts of TiO_2 NPs with nylon-6 solution. The addition of a small amount of TiO_2 NPs improves the hydrophilicity and mechanical strength of nylon-6 nanofiber mats, and it was able to form a high aspect ratio spider-net like nanostructure. The enhanced hydrophilicity of the spider-net like mats can decrease the antifouling effect to make the mat a potential candidate for water filtration. The TiO_2 entrapped nylon-6 mat showed better bactericidal and UV blocking ability as compared to the neat nylon-6 mat under UV light. This high aspect ratio nanofiber mat (due to the spider-net like structure) can be potentially applicable in a wide variety of filter applications ranging from air purification media to water filter media as well as different kinds of protective clothing.

Acknowledgments

This research work was supported by the Korean Research Foundation Grant funded by Korea government (MOEHRD) (KRF–2005-210-D00042) and the Regional Research Centers Programs of the Korean Ministry of Education & Human Resource Development through the Center for Healthcare Technology Development, Chonbuk National University, Jeonju 561-756, Republic of Korea. We thank Mr. Jong-Gyun Kang and Miss Lee Jeong Ok, Centre for University Research Facility, for taking high-quality TEM images.

References

[1] J. Jordan, K.I. Jacob, R. Tannenbaum, M.A. Sharaf, I. Jasiuk, Experimental trends in polymer nanocomposites—a review, Mater. Sci. Eng. A 393 (2005) 1–11.
[2] V. Viswanathan, T. Laha, K. Balani, A. Agarwal, S. Seal, Challenges and advances in nanocomposite processing techniques, Mater. Sci. Eng. R 54 (2006) 121–285.
[3] R.A. Damodar, S.J. You, H.H. Chou, Study the self cleaning, antibacterial and photocatalytic properties of TiO_2 entrapped PVDF membranes, J. Hazard. Mater. 172 (2009) 1321–1328.
[4] K.M. Yun, C.J. Hogan, Y. Matsubayashi, M. Kawabe, F. Iskandar, K. Okuyama, Nanoparticle filtration by electrospun polymer fibers, Chem. Eng. Sci. 62 (2007) 4751–4759.
[5] J.A. Lee, K.C. Krogman, M. Ma, R.M. Hill, P.T. Hammond, G.C. Rutledge, Highly reactive multilayer-assembled TiO_2 coating on electrospun polymer nanofibers, Adv. Mater. 21 (2009) 1252–1256.
[6] P. Raghavan, X. Zhao, J.K. Kim, J. Manuel, G.S. Chauhan, J.H. Ahn, C. Nan, Ionic conductivity and electrochemical properties of nanocomposite polymer electrolytes based on electrospun poly(vinylidene fluoride-co-hexafluropropylene) with nano-sized ceramics fillers, Elec. Acta. 54 (2008) 228–234.

[7] F. Yang, S.K. Both, X. Yang, X.F. Walboomers, J.A. Jansen, Development of an electrospun nano-apatite/PCL composite membrane for GTR/GBR application, Acta. Biomater. 5 (2009) 3295–3304.
[8] F. Yang, J.G.C. Wolke, J.A. Jansen, Biomimetic calcium phosphate coating on electrospun poly(e-caprolactone) scaffolds for bone tissue engineering, Chem. Eng. J. 137 (2008) 154–161.
[9] T. Rajesh, D. Ahujab, Kumarb, Recent progress in the development of nano-structured conducting polymers/nanocomposites for sensor applications, Sens. Actutators B 136 (2009) 275–286.
[10] L. Malfatti, M.G. Bellino, P. Innocenzi, G.J.A.A. Soler-Illia, One-pot route to produce hierarchically porous titania thin films by controlled self-assembly, swelling, and phase separation, Chem. Mater. 21 (2009) 2763–2769.
[11] B. Chi, T. Jin, Synthesis of Titania nanostructure films via $TiCl_4$ evaporation-deposition route, Cryst. Growth Des. 7 (2007) 815–819.
[12] V.R. Koganti, D. Dunphy, V. Gowrishankar, M.D. McGehee, X. Li, J. Wang, S.E. Rankin, Generalized coating route to silica and titania films with orthogonally tilted cylindrical nanopore arrays, Nano Lett. 6 (2006) 2567–2570.
[13] N.A.M. Barakat, M.F. Abadir, F.A. Sheikhd, M.A. Kanjwal, S.J. Park, H.Y. Kim, Polymeric nanofibers containing solid nanoparticles prepared by electrospinning and their applications, Chem. Eng. J. 156 (2010) 487–495.
[14] D. Kimmer, P. Slobodian, D. Petras, M. Zatloukal, R. Olejnik, P. Saha, Polyurethane/multiwalled carbon nanotube nanowebs prepared by an electrospinning process, J. Appl. Polym. Sci. 111 (2009) 2711–2714.
[15] B. Ding, L. Chunrong, M. Yasuhiro, O. Kuwaki, S. Shiratori, Formation of novel 2D polymer nanowebs via electrospinning, Nanotechnology 17 (2006) 3685–3691.
[16] H.R. Pant, M.P. Bajgai, K.T. Nam, K.H. Chu, S.J. Park, H.Y. Kim, Formation of electrospun nylon-6/methoxy poly(ethylene glycol) oligomer spider-wave nanofibers, Mater. Lett. 64 (2010) 2087–2090.
[17] D.C. Parajuli, M.P. Bajgai, J.A. Ko, H.K. Kang, M.S. Khil, H.Y. Kim, Synchronized polymerization and fabrication of poly(acrylic acid) and nylon hybrid mats in electrospinning, ACS Appl. Mater. Interf. 1 (2009) 750–757.
[18] N.A.M. Barakat, M.A. Kanjwal, F.A. Sheikh, H.Y. Kim, Spider-net within the N6, PVA and PU electrospun nanofibers mats using salt addition: novel strategy in the electrospinning process, Polymer 50 (2009) 4389–4396.
[19] J.L. Pey, Corrosion protection of pipes, fittings and component pieces of water treatment and pumping stations, Anti-Cor. Meth. Mater. 44 (1997) 94–99.
[20] D. Aussawasathien, C. Teerawattananon, A. Vongachariya, Separation of micron to sub-micron particles from water: electrospun nylon-6 nanofibrous membranes as pre-filters, J. Membr. Sci. 315 (2008) 11–19.
[21] A.L. Linsebigler, G. Lu, J.T. Yates, Review-photocatalysis on TiO_2 surfaces: principles, mechanisms, and selected results, Chem. Rev. 95 (3) (1995) 735–758.
[22] M.R. Hoffmann, S.T. Martin, W. Choi, D.W. Bahnemann, Environmental applications of semiconductor photocatalysis, Chem. Rev. 95 (1) (1995) 69–96.
[23] A. Fujishima, K. Honda, Electrochemical photolysis of water at a semiconductor electrode, Nature 238 (1972) 37–38.
[24] K. Nagaveni, G. Sivalingam, M.S. Hegde, G. Madras, Photocatalytic degradation of organic compounds over combustion-synthesized nano-TiO_2, Environ. Sci. Technol. 38 (2004) 1600–1604.
[25] M.I. Mejia, J.M. Marin, G. Restrepo, C. Pulgarin, E. Mielczarski, J. Mielczarski, I. Stolitchnov, J. Kiwi, Innovative UVC light (185 nm) and radio-frequency-plasma pretreatment of nylon surfaces at atmospheric pressure and their Implications in photocatalytic processes, ACS Appl. Mater. Interf. 1 (2009) 2190–2198.
[26] J.R. Schaefgen, C.F. Trivisonno, Polyelectrolyte behavior of polyamides. I. Viscosities of solutions of linear polyamides in formic acid and sulfuric acid, J. Am. Chem. Soc. 73 (1951) 4580–4585.
[27] S.K. Lim, S.K. Lee, S.H. Hwang, H. Kim, Photocatalytic deposition of silver nanoparticles onto organic/inorganic composite nanofibers, Macro. Mater. Eng. 291 (2006) 1265–1270.
[28] D. Shah, P. Maiti, D.D. Jiang, C.A. Batt, E.P. Giannelis, Effect of nanoparticle mobility on toughness of polymer nanocomposites, Adv. Mater. 17 (2005) 525–528.
[29] Y. Yang, H. Zhang, P. Wang, Q. Zheng, J. Li, The influence of nano-sized TiO_2 fillers on the morphologies and properties of PSF UF membrane, J. Memb. Sci. 288 (2007) 231–238.
[30] J. Kiwi, V. Nadtochenko, New evidence for TiO_2 photocatalysis during bilayer lipid peroxidation, J. Phys. Chem. B 108 (2004) 17675–17684.
[31] J. Kiwi, V. Nadtochenko, Evidence for the mechanism of photocatalytic degradation of the bacterial wall membrane at the TiO2 interface by ATR-FTIR and laser kinetic spectroscopy, Langmuir 21 (2005) 4631–4641.